On-demand source of maximally entangled photon pairs using the biexciton-exciton radiative cascade

R. Winik,[1,2] D. Cogan,[2] Y. Don,[2] I. Schwartz,[2] L. Gantz,[2] E. R. Schmidgall,[2] N. Livneh,[3]
R. Rapaport,[3] E. Buks,[1] and D. Gershoni[2,*]

[1]*Andrew and Erna Viterbi Department of Electrical Engineering, Technion, Haifa 32000, Israel*

[2]*The Physics Department and the Solid State Institute, Technion–Israel Institute of Technology, 32000 Haifa, Israel*

[3]*Applied Physics Department, The Benin School of Computer Sciences and Engineering, The Hebrew University, Jerusalem 91904, Israel*

(Received 14 March 2017; revised manuscript received 11 May 2017; published 28 June 2017)

We perform full time-resolved tomographic measurements of the polarization state of pairs of photons emitted during the radiative cascade of the confined biexciton in a semiconductor quantum dot. The biexciton was deterministically initiated using a π-area pulse into the biexciton two-photon absorption resonance. Our measurements demonstrate that the polarization states of the emitted photon pair are maximally entangled. We show that the measured degree of entanglement depends solely on the temporal resolution by which the time difference between the emissions of the photon pair is determined. A route for fabricating an on-demand source of maximally polarization entangled photon pairs is thereby provided.

DOI: 10.1103/PhysRevB.95.235435

The ability to generate entangled photons on demand is crucial for many future applications in quantum information processing. Devices based on the biexciton-exciton radiative cascade in a single semiconductor quantum dot (QD) are considered to be one of the best candidates for these applications [1–3]. The ability to deterministically excite the biexciton using its two-photon absorption resonance [4,5] makes this avenue even more promising. A remaining challenge, however, is the excitonic fine structure, which splits the two exciton eigenstates, thus providing spectral "which-path" information on the radiative cascade and preventing the pairs of emitted photons from being polarization entangled [2]. Various strategies were tried in an attempt to reduce the influence of the fine structure splitting, such as spectral [2] and temporal filtering [2,6], which introduced nondesired, nondeterministic post-selection, and enhancement of the radiative rate using the Purcell effect [3], thereby reducing but not limiting the effect of exciton precession. Attempts to reduce the fine-structure splitting using heat treatment [7] or growth along the [111] crystalographic direction [8] were reported as well as applications of external stress [9] and electric [10] and magnetic field tuning [11,12]. These efforts often result in unwanted loss of emission quantum efficiency [10] and increase in the exciton spin decoherence [6].

We present here a study of a single semiconductor quantum dot, optically depleted [13] and then resonantly excited on demand by a π-area pulse to the biexciton two-photon absorption resonance [5]. The resulting pairs of biexciton and exciton photons are detected by two superconducting detectors synchronized to the exciting laser pulse. By performing synchronized time-resolved polarization tomography of the two emitted photons, we unambiguously show that the photons remain maximally polarization entangled during the whole radiative decay, and that the measured degree of entanglement does not depend on the QD source, but rather depends on the temporal resolution by which the time difference between the two photon emissions can be determined. Since during the radiative decay the exciton does not lose coherence, there is no need to eliminate the excitonic fine structure splitting. A relatively simple arrangement [14,15] should therefore provide a reliable source of on-demand pairs of maximally entangled photons from a single quantum dot, regardless of its nonvanishing excitonic fine structure splitting.

I. THEORETICAL BACKGROUND

The biexciton-exciton radiative cascade is schematically described in Fig. 1(a). In the figure, resonant excitation of the biexciton using a π-area pulse to the virtual two-photon excitation (TPE) resonance [5,16–18] is described by an upward green arrow. The power required to achieve the TPE π pulse (2.53 μW) is about an order of magnitude larger than that required for the exciton (0.25 μW), in agreement with Ref. [17]. At this power level, no residual absorption off the TPE resonance was observed, indicating negligible free carrier photogeneration. The 12 ps long resonant TPE pulse follows a few nanosecond long optical depletion pulse [13] which empties the QD of charges and long-lived dark excitons. The π-area pulse therefore deterministically photogenerates a confined ground state biexciton ($|XX^0\rangle$) in the QD [5,16]. The biexciton spontaneously radiatively decays, leaving in the QD an exciton in a coherent superposition of its two eigenstates: the $|X^0_H\rangle$ and the $|X^0_V\rangle$ states [19,20]. The optical selection rules for the biexciton radiative recombination and the lack of information by "which path" the recombination proceeds result in entanglement between the exciton state and the polarization state of the emitted photon [21–23]. Their mutual wave function is given by

$$\left|\psi_{P_1X^0}\right\rangle = \frac{1}{\sqrt{2}}\left(\left|H_1X^0_H\right\rangle + \left|V_1X^0_V\right\rangle\right), \tag{1}$$

where $|H_1\rangle$ and $|V_1\rangle$ are the two rectilinear polarization states of the first (biexciton) photon. Since the two exciton eigenstates are not degenerate, the relative phase between these eigenstates precesses in time with a period of $T_P = h/\Delta$, where h is the Planck constant and Δ is the exciton fine

*dg@physics.technion.ac.il

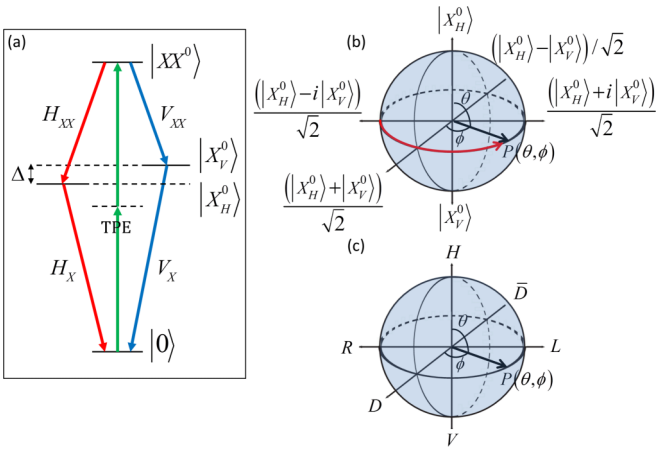

FIG. 1. (a) Schematic description of the energy levels and optical transitions involved in the biexciton two-photon resonant excitation (TPE) and its radiative decay cascade. (b) The exciton Bloch sphere. The red arrow describes precession of a coherent superposition of its two eigenstates the X_H^0 and the X_V^0. (c) The photon polarization Poincaré sphere.

structure splitting [see Fig. 1(a)]. This precession is schematically described on the exciton Bloch sphere in Fig. 1(b). The precession "stops" when the exciton recombines and the radiative cascade is completed with the emission of a second photon. The two photons are thus entangled. Their mutual wave function depends on the recombination time and is given by

$$\left|\psi_{P_1P_2}(t)\right\rangle = \frac{1}{\sqrt{2}}\left(|H_1H_2\rangle + e^{-i2\pi\frac{t}{T_P}}|V_1V_2\rangle\right), \tag{2}$$

where $|H_2\rangle$ and $|V_2\rangle$ are the second (exciton) photon polarization states and $t = t_{X^0} - t_{XX^0}$ is the time between the emission of the biexciton photon t_{XX^0} and that of the exciton t_{X^0}. It follows that the normalized two-photon polarization density matrix is expressed in the basis $|H_1H_2\rangle$, $|H_1V_2\rangle$, $|V_1H_2\rangle$, and $|V_1V_2\rangle$ as

$$\rho_{P_1P_2}(t) = \frac{1}{2}\begin{pmatrix} 1 & 0 & 0 & e^{-i2\pi\frac{t}{T_P}} \\ 0 & 0 & 0 & 0 \\ 0 & 0 & 0 & 0 \\ e^{i2\pi\frac{t}{T_P}} & 0 & 0 & 1 \end{pmatrix}. \tag{3}$$

To evaluate the degree of entanglement between the two photon polarization states we used a standard measure: the negativity $\mathcal{N}$ of their polarization density matrix [24], where $\mathcal{N}$ is defined as the magnitude of the negative eigenvalue of the partially transposed density matrix. For $\mathcal{N} > 0$, the two photons are entangled with a fidelity of about $2\mathcal{N}$ to a two-photon Bell state. $\mathcal{N} = \frac{1}{2}$ corresponds to maximal entanglement with unit fidelity to a two-photon Bell state. It is easy to see from Eq. (3) that the negativity of the two-photon density matrix is given by

$$\mathcal{N}[\rho_{P_1P_2}(t)] = \tfrac{1}{2}\left|e^{i\frac{\Delta}{\hbar}t}\right| = \tfrac{1}{2}\left|e^{i2\pi\frac{t}{T_P}}\right| = \tfrac{1}{2}. \tag{4}$$

and thus the two photon polarization states are always maximally entangled. The information contained in the different colors of the photon pairs, which reveals the decay path of the radiative cascade, remains in the temporal dependence of the phase of the nondiagonal elements of the polarization density matrix.

In an actual experiment, the temporal resolution is limited. Thus, if one cannot define the time difference between the two photons to a better resolution than ΔT, the negativity in the measured polarization density matrix is given by

$$\mathcal{N}\left[\rho_{P_1P_2}(t,\Delta T)\right] = \frac{1}{2\Delta T}\left|\int_t^{t+\Delta T} e^{i2\pi\frac{t'}{T_P}}\,dt'\right|, \tag{5}$$

where for simplicity we assumed that the temporal resolution is represented by a square temporal window of width ΔT. It follows that the measured negativity is independent of the time t:

$$\mathcal{N}\left[\rho_{P_1P_2}(\Delta T)\right] = \frac{1}{2}\left|\mathrm{sinc}\left(\pi\frac{\Delta T}{T_P}\right)\right|. \tag{6}$$

As can be seen from Eq. (6), the negativity and hence the measured degree of entanglement vanish for $\Delta T = T_P$, but they revive before vanishing for a wider temporal window ($\Delta T \gg T_P$).

We define a general polarization state of light as a point on the Poincaré sphere in which the horizontal, $|H\rangle$ (vertical, $|V\rangle$) rectilinear polarization forms the north (south) pole of the unit sphere as shown in Fig. 1(c) [25]. Thus any polarization can be described in terms of the rectilinear basis using two angles θ and ϕ:

$$|P(\theta,\phi)\rangle = \cos(\theta/2)\,|H\rangle + e^{i\phi}\sin(\theta/2)|V\rangle. \tag{7}$$

In this representation, the rectilinear polarization basis is given by

$$|H\rangle = |P(\theta=0,\phi)\rangle, \quad |V\rangle = |P(\theta=\pi,\phi\rangle, \tag{8}$$

and two additional orthogonal bases, the diagonal linear and the circular polarization bases, are given by

$$\begin{aligned} |D\rangle &= (|H\rangle + |V\rangle)/\sqrt{2} = |P(\theta=\pi/2,\phi=0)\rangle, \\ |\bar{D}\rangle &= (|H\rangle - |V\rangle)/\sqrt{2} = |P(\theta=\pi/2,\phi=\pi)\rangle \end{aligned} \tag{9}$$

and

$$\begin{aligned} |L\rangle &= (|H\rangle + i\,|V\rangle)/\sqrt{2} = |P(\theta=\pi/2,\phi=\pi/2)\rangle, \\ |R\rangle &= (|H\rangle - i\,|V\rangle)/\sqrt{2} = |P(\theta=\pi/2,\phi=3\pi/2)\rangle. \end{aligned} \tag{10}$$

These bases are schematically described in Fig. 1(c).

Once the first photon is detected, then the probability rate to detect the first photon with polarization P_1 and the second cascading photon in polarization P_2 at time t later is given by

$$\begin{aligned} &p[t,P_1(\theta_1,\phi_1),P_2(\theta_2,\phi_2)] \\ &\quad = p_{X^0}(t)\left|\langle P_1P_2|\psi_{P_1P_2}(t)\rangle\right|^2 \\ &\quad = \frac{e^{-\frac{t}{\tau_R}}}{2\tau_R}\left|\cos\frac{\theta_1-\theta_2}{2}\cos\left(\frac{\phi_1+\phi_2}{2}+\frac{\pi t}{T_P}\right)\right. \\ &\qquad \left. + i\cos\frac{\theta_1+\theta_2}{2}\sin\left(\frac{\phi_1+\phi_2}{2}+\frac{\pi t}{T_P}\right)\right|^2, \end{aligned} \tag{11}$$

where $p_{X^0}(t) = e^{-\frac{t}{\tau_R}}/\tau_R$ is the recombination rate of the exciton and τ_R is the exciton radiative lifetime. Note that

TABLE I. Various two-photon polarization-sensitive emission probability rates.

Criteria	No. of cases	$p(t,P_1,P_2)/p_{X^0}(t)$
$\theta_1=\theta_2=0(\pi)$	2	$\frac{1}{2}$
$\theta_1=\pi(0),\theta_2=0(\pi)$	2	0
$\theta_1=0\,\text{or}\,\pi,\theta_2=\pi/2$	8	$\frac{1}{4}$
$\theta_1=\pi/2,\theta_2=0\,\text{or}\,\pi$	8	$\frac{1}{4}$
$\theta_1=\theta_2=\pi/2$	16	$\frac{1}{4}[1+\cos(\phi_1+\phi_2+2\pi\frac{t}{T_P})]$

the probability P_{HH} (P_{VV}) that the QD emits both photons co-linearly polarized, H (V), is given by

$$P_{HH(VV)}=\int_0^\infty p[t',HH(VV)]dt'=\frac{1}{2}, \qquad (12)$$

as expected for an on-demand generated biexciton radiative cascade. The probability to detect the two photons in a given polarization state $P^D_{P_1P_2}$ is given by $P^D_{P_1P_2}=\eta^2 P_{P_1P_2}$, where η is the light harvesting efficiency of our experimental system [26].

For polarization tomography measurements one detects two photons, which temporally belong to the same cascade, and projects the polarization state of each photon on the three orthogonal polarization bases. In at least one of the bases, two measurements on both polarization states are required. Thus $4\times4=16$ independent time-resolved polarization-sensitive two-photon correlation measurements are needed in order to fully characterize the temporal evolution of the two photons' polarization density matrix [27]. Considering only the polarization bases of Eqs. (8)–(10), one gets 36 possible different two-photon polarization-sensitive probability rates, which divide essentially to 4 different cases (see Table I). In the 16 cases where $\theta_1=\theta_2=\pi/2$ oscillatory temporal dependence of the probability rate is expected with a relative phase which is given by $\phi_1+\phi_2$.

The sample was grown by molecular beam epitaxy on [001]-oriented GaAs substrate. A layer of strain-induced InAs QDs was deposited in the center of an intrinsic GaAs layer. The GaAs layer was placed between two AlAs/GaAs distributed Bragg mirrors of quarter wavelength, facilitating a microcavity. The microcavity design provides efficient collection of the light emitted due to recombination of QD confined electrons and holes from their respective lower energy levels. The QD is resonantly excited to the two-photon biexciton absorption resonance using a synchronously pumped dye laser pulse with a repetition rate of 76 MHz. The temporal width of the laser pulse is ~12 ps and the spectral width is ~100 μeV. The resulting two-photon emission is measured using a polarization selective Hanbury Brown–Twiss (HBT) arrangement as schematically described in Fig. 2(a). The emitted photoluminescence (PL) is divided by a nonpolarizing beam splitter into two separated beams. A pair of liquid-crystal variable retarders (LCVR) and a polarizing beam splitter on each beam is used to project the light on the desired polarization direction. The energy of the collected light on each beam is then filtered by a 1 meter long monochromator (MC) followed by a superconducting nanowire single-photon detector (SNSPD) and a time-correlated single-photon counter (TCSPC).

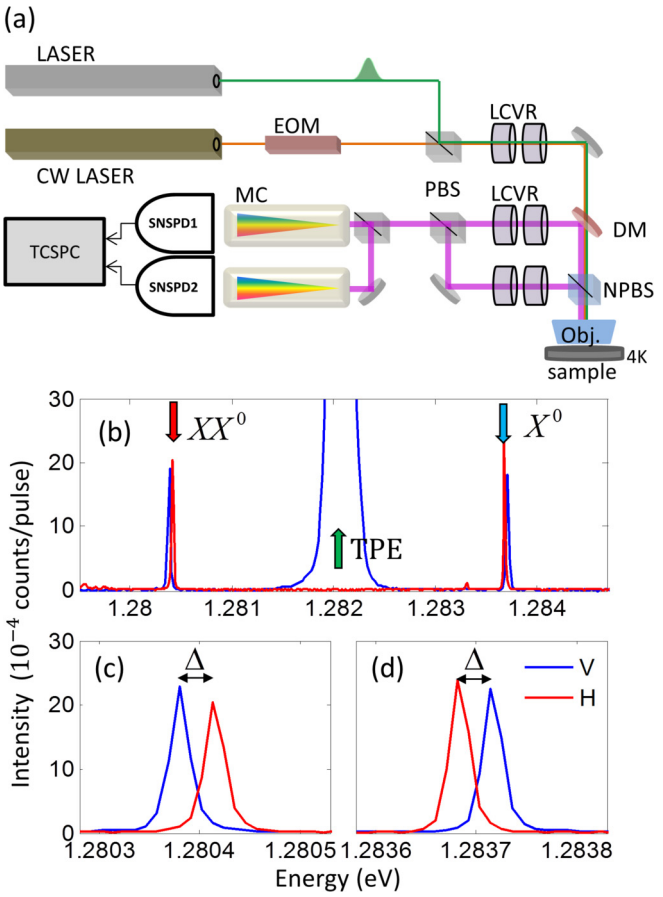

FIG. 2. (a) Schematic description of the experimental system. (b) Polarization-sensitive photoluminescence spectra of the biexciton-exciton radiative cascade under pulsed excitation into the two-photon absorption resonance of the biexciton. Note that for this particular measurement the laser was rectilinearly vertically polarized. (c) [(d)] expanded energy scale spectra for the biexciton (XX^0) [exciton (X^0)] spectral lines. (Abbreviations: PBS - polarizing beam splitter, MC - monochromator, SNSPD - superconducting nanowire single photon detector, LCVR - liquid crystal variable retarder, TCSPC - time-correlated single photon counter, EOM - electro-optic modulator, DM - dichroic mirror.)

II. RESULTS

In Fig. 2(b) we present polarization-sensitive PL spectra of the photoluminescence from the QD under resonant excitation into the biexciton two-photon absorption resonance [5,16]. The energy of the exciting laser is tuned exactly between the XX^0 and X^0 spectral line energies. Each of these spectral lines is composed of two cross linearly polarized components split by $\Delta=34$ μeV, as can be clearly seen in Figs. 2(c) and 2(d), which present the X^0 and XX^0 spectral lines, respectively, on expanded energy scales. This energy splitting translates into an exciton precession time of $T_P=h/\Delta=122$ ps.

Our setup was carefully designed to facilitate polarization-sensitive time-resolved correlation measurements between photons emitted from the XX^0 and the X^0 spectral lines. The correlation measurements were performed after deterministic generation of the XX^0 biexciton using a π-area pulse resonantly tuned into the biexciton two-photon absorption

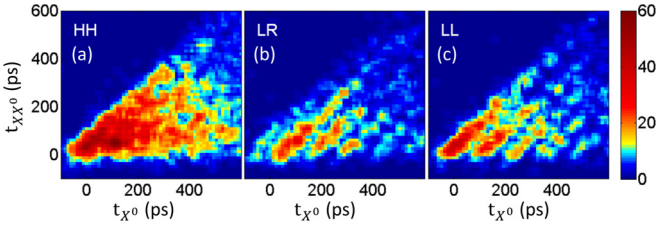

FIG. 3. The number of events (given by the color bar to the right) in which a biexciton and an exciton photons are detected as a function of their detection times as measured from the time of the pulsed excitation. In (a) the two photons are co-linearly polarized, H, in (b) they are cross-circularly polarized (the biexciton L and the exciton R), and in (c) they are co-circularly polarized, L.

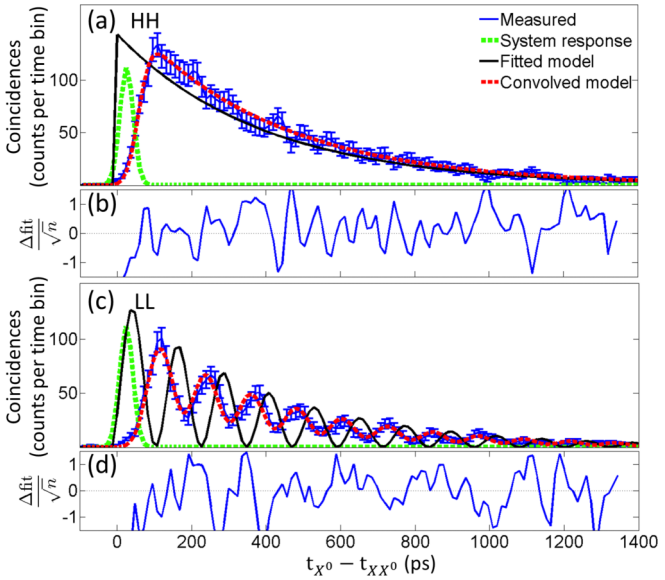

FIG. 4. (a) The solid green line represents the measured temporal response function of the system. The blue marks with error bars represent the measured number of co-rectilinearly polarized two-photon detection events as a function of the difference between their detection times. The black solid line represents the best fitted Eq. (11) [which for this polarization projections is given by $\frac{1}{2}p_{X^0}(t)$] and red solid line represents the model convolved by the system response function. (b) The difference between the convolved model and the measured data normalized by the experimental uncertainty. The quality of the fit is evident by the fact that the magnitude of the normalized difference does not exceed unity considerably. (c) and (d) are similar to (a) and (b), respectively, but for co-circularly polarized two-photon events [note that in this case Eq. (11) is $\frac{1}{4}[1-\cos(\frac{2\pi t}{T_P})]p_{X^0}(t)$].

resonance [5,16]. Prior to the generating pulse, a 4 ns long depletion pulse was used [13], verifying that the QD is empty from charges and dark excitons, ready for biexciton generation. The depletion pulse was produced using a continuous wave Ti:sapphire laser light, temporally shaped by an electro-optical modulator (EOM). The modulator was synchronized to the pulsed, synchronously pumped ps dye laser, which generated the biexciton [see Fig. 2(a)]. We note here that, for on-demand generation of the biexciton by two photon absorption, the QD must be *a priori* emptied from long-lived charges and dark excitons, which will prevent absorption. The depletion pulse provides this condition, as verified by measuring the intensity of the exciton emission and comparing it to the expected emission rate of one photon per laser pulse (calibrated by the known light harvesting efficiency of our system [26]). The optical depletion may be replaced by a faster reverse bias electrical pulse, but the on-demand biexciton generation cannot be achieved by nonresonant electrical injection [28].

In Fig. 3 the correlation measurements are presented as two-dimensional images showing by the false color scale the number of events in which two photons are detected as a function of their detection times after the excitation pulse. For these measurements the monochromators' slits were broadly opened in order to collect all the emitted photons from both spectral lines. The spectral window width under these conditions was about an order of magnitude wider than the excitonic fine structure splitting. Figure 3(a) shows the events when the two photons are H linearly copolarized. Figures 3(b) and 3(c), show the events when the two photons are cross- and co-circularly polarized, respectively. Fifteen more similar maps (not shown) were measured for different combinations of the two photon polarizations, providing the data required for constructing the temporal evolution of the two-photon polarization density matrix. The temporal evolution of the signal integrated over the exciton detection time t_{X^0} showed polarization-independent simple exponential decay with a characteristic biexciton decay time of 260 ± 10 ps (not shown). Therefore, in order to increase the measurement statistics, we summed over the detection times of the biexciton t_{XX^0} in Fig. 3 and obtained the number of coincidences as a function of the time difference between the photon detections.

Typical measurements are presented by the blue symbols and error bars in Fig. 4. In Fig. 4(a) the integrated data from Fig. 3(a) where the two photons are H co-linearly polarized are presented, and in Fig. 4(c) the data are obtained from Fig. 3(c) where the two photons are co-circularly polarized. In both figures, the green solid line presents the system temporal response as obtained by detecting the picosecond laser pulse, on both detectors. The system response is best-fitted by a Gaussian function with full width at half maximum of 42 ps.

The solid black lines in Figs. 4(a) and 4(c) represent the best fitted calculations using Eq. (11). We note here that in fitting all the 16 different polarization-sensitive correlation measurements, only one fitting parameter was used: τ_R, the radiative lifetime of the exciton. We used $\tau_R = 410 \pm 10$ ps. The exciton precession period of $T_P = 122 \pm 12$ ps was directly obtained from the spectral measurement of the exciton fine structure. Since all the correlation measurements were performed together, as the system automatically changed the polarization projections every minute, all the curves are automatically normalized and no attempt was made to fit their relative intensities. The overall coincidence accumulation rate of about 10^{-6} coincidences per pulse was also in agreement with the known light harvesting efficiency of our experimental setup [26]. The solid black lines represent the calculations using Eq. (11). The red lines overlaying the data are obtained by convolving the calculations by the system response function. Figures 4(b) and 4(d) show the difference between the data and the convolved calculations. These differences are within

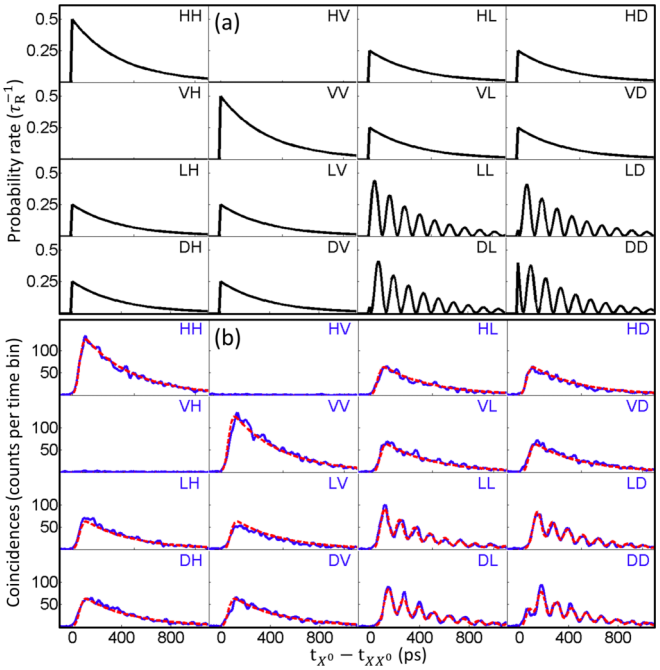

FIG. 5. Sixteen different polarization-sensitive two-photon detection coincidences as a function of the time difference between the detection of the first and second photon. Solid black lines in (a) represent the calculated probability rates using Eq. (11). Solid blue lines in (b) represent the measured coincidences rates, and solid red lines in (b) represent the calculated probability rates convolved by the measured system temporal response as shown in Fig. 4. The first (second) capital letter above each curve represents the polarization on which the biexciton (exciton) photon was projected.

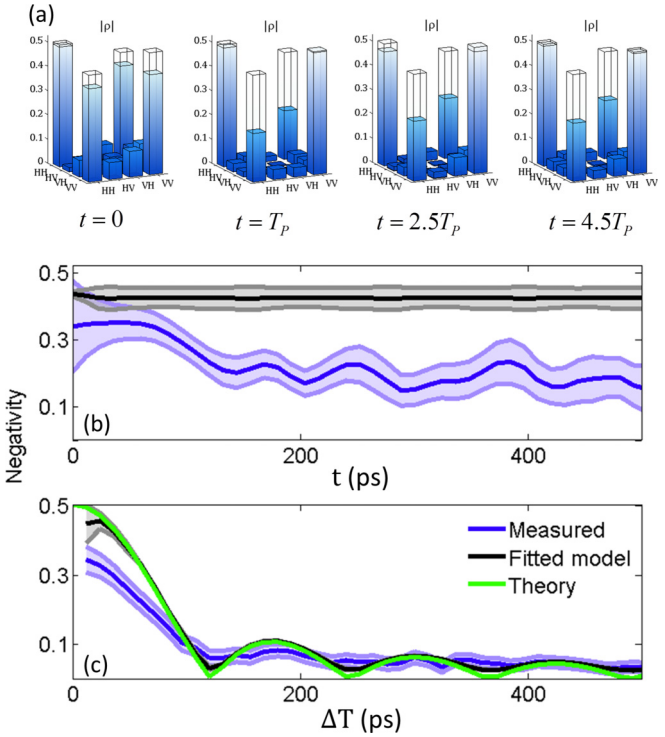

FIG. 6. (a) the absolute value of the two-photon polarization density matrix for various times after the detection of the biexciton photon. Blue bars represent matrix elements obtained directly from the measured data, while empty bars represent matrix elements deduced from the fitted calculations, which consider the measured temporal response of the detectors. In both cases the temporal window width over which the data is integrated was set to $\Delta T = 24$ ps. (b) The negativity of the two photon polarization density matrix as a function of the time difference between the exciton and biexciton detection times for temporal window width of $\Delta T = 24$ ps. The blue line presents the negativity deduced directly from the measured raw data. The black line presents the negativity deduced from the fitted calculations considering the system response. (c) The negativity of the two photons' polarization density matrix as a function of the temporal window width, ΔT. The blue line presents the negativity deduced directly from the measured raw data. The black line presents the negativity deduced from the fitted calculations, considering the system response. The theoretical dependence calculated by Eq. (6) is represented by the green solid line. Shaded areas with corresponding colors in both (b) and (c) represent experimental uncertainties of one standard deviation.

the experimental uncertainty and imply excellent agreement between the measured data and the convolved calculations.

In Fig. 5(a) we present by solid black lines 16 different polarization-sensitive time-resolved probability rates calculated using Eq. (11) (or Table I). These 16 different polarization projections are required for tomographic reconstruction of the two photon polarization density matrix. For these calculations we used $T_P = h/\Delta = 122$ ps as deduced from the PL spectra, and $\tau_R = 410$ ps as the only fitted parameter. In Fig. 5(b) solid blue lines represent the corresponding 16 time-resolved two-photon coincidence rate measurements. Solid red lines in (b) overlaid on the measured data represent the calculations of Fig. 5(a) convolved with the system response function from Figs. 4(a) and 4(c). As can be seen in Fig. 5(b), the agreement between the calculations and measurements is excellent.

The two-photon density matrix as function of time was reconstructed [27] both from the measured data and from the model calculations only. The absolute values of four such matrices for various time differences after the detection of the biexciton photon are presented in Fig. 6(a). In both cases, the temporal window width, ΔT, over which the data was integrated was set to 24 ps. In Fig. 6(a), blue bars represent the measured [deduced from the data in Fig. 5(b)] absolute values of the density matrix elements. Empty bars represent the matrix elements obtained from the fitted model calculations [deduced from Fig. 5(b)], which consider the measured temporal response of our detectors.

The negativity of the density matrix as a function of time between the photons is presented in Fig. 6(b), in blue for the as-measured matrices and in black for the calculated ones, considering the detectors temporal response. Here as well, the temporal window width ΔT was set to 24 ps.

Figure 6(c) presents the negativity of the two-photon polarization density matrix as a function of the temporal window width, ΔT. The solid blue line in the figure presents the negativity as deduced directly from the measured raw data. The solid black line presents the negativity deduced from the fitted calculations, considering the detectors temporal response. Shaded areas with corresponding colors in both Figs. 6(b) and 6(c) represent uncertainties of one standard

deviation. Note the excellent agreement between the solid black line and the theoretical dependence predicted by Eq. (6), represented in Fig. 6(c) by the green solid line.

III. SUMMARY

In summary, we have demonstrated experimentally that the biexciton-exciton radiative cascade in semiconductor quantum dots is an excellent deterministic source of maximally polarization entangled photon pairs. We showed that (a) the polarization states of the emitted two photons are maximally entangled during the whole radiative decay, and (b) the measured degree of entanglement between the polarization states of the two photons depends only on the temporal resolution by which the time difference between the two photon emissions is determined. A relatively simple arrangement, which provides periodic retardation change compatible with the exciton precession period, can therefore transform any quantum dot into an on-demand source of maximally entangled photons [14,15,29].

ACKNOWLEDGMENTS

We thank N. H. Lindner, O. Kenneth, and J. A. Avron for helpful discussions and P. M. Petroff for the sample. The support of the Israeli Science Foundation (ISF), the Technion's RBNI and the Israeli Focal Technology Area on "Nanophotonics for Detection" is gratefully acknowledged. This project has also received funding from the European Research Council (ERC) under the European Union's Horizon 2020 Research and Innovation Programme (Grant Agreement No. 695188).

[1] O. Benson, C. Santori, M. Pelton, and Y. Yamamoto, Regulated and Entangled Photons from a Single Quantum Dot, Phys. Rev. Lett. **84**, 2513 (2000).

[2] N. Akopian, N. H. Lindner, E. Poem, Y. Berlatzky, J. Avron, D. Gershoni, B. D. Gerardot, and P. M. Petroff, Entangled Photon Pairs from Semiconductor Quantum Dots, Phys. Rev. Lett. **96**, 130501 (2006).

[3] A. Dousse, J. Suffczynski, A. Beveratos, O. Krebs, A. Lemaitre, I. Sagnes, J. Bloch, P. Voisin, and P. Senellart, Ultrabright source of entangled photon pairs, Nature (London) **466**, 217 (2010).

[4] S. Bounouar, M. Müller, A. M. Barth, M. Glässl, V. M. Axt, and P. Michler, Phonon-assisted robust and deterministic two-photon biexciton preparation in a quantum dot, Phys. Rev. B **91**, 161302 (2015).

[5] M. Müller, S. Bounouar, K. D. Jöns, M. Glässl, and P. Michler, On-demand generation of indistinguishable polarization-entangled photon pairs, Nat. Photon. **8**, 224 (2014).

[6] R. M. Stevenson, A. J. Hudson, A. J. Bennett, R. J. Young, C. A. Nicoll, D. A. Ritchie, and A. J. Shields, Evolution of Entanglement Between Distinguishable Light States, Phys. Rev. Lett. **101**, 170501 (2008).

[7] R. J. Young, R. M. Stevenson, A. J. Shields, P. Atkinson, K. Cooper, D. A. Ritchie, K. M. Groom, A. I. Tartakovskii, and M. S. Skolnick, Inversion of exciton level splitting in quantum dots, Phys. Rev. B **72**, 113305 (2005).

[8] M. A. M. Versteegh, M. E. Reimer, K. D. Jöns, D. Dalacu, P. J. Poole, A. Gulinatti, A. Giudice, and V. Zwiller, Observation of strongly entangled photon pairs from a nanowire quantum dot, Nat. Commun. **5**, 5298 (2014).

[9] J. Zhang, J. S. Wildmann, F. Ding, R. Trotta, Y. Huo, E. Zallo, D. Huber, A. Rastelli, and O. G. Schmidt, High yield and ultrafast sources of electrically triggered entangled-photon pairs based on strain-tunable quantum dots, Nat. Commun. **6**, 10067 (2015).

[10] A. J. Bennett, M. A. Pooley, R. M. Stevenson, M. B. Ward, R. B. Patel, A. B. de La Giroday, N. Sköld, I. Farrer, C. A. Nicoll, D. A. Ritchie *et al.*, Electric-field-induced coherent coupling of the exciton states in a single quantum dot, Nat. Phys. **6**, 947 (2010).

[11] R. J. Young, R. M. Stevenson, P. Atkinson, K. Cooper, D. A. Ritchie, and A. J. Shields, Improved fidelity of triggered entangled photons from single quantum dots, New J. Phys. **8**, 29 (2006).

[12] R. M. Stevenson, R. J. Young, P. See, D. G. Gevaux, K. Cooper, P. Atkinson, I. Farrer, D. A. Ritchie, and A. J. Shields, Magnetic-field-induced reduction of the exciton polarization splitting in InAs quantum dots, Phys. Rev. B **73**, 033306 (2006).

[13] E. R. Schmidgall, I. Schwartz, D. Cogan, L. Gantz, T. Heindel, S. Reitzenstein, and D. Gershoni, All-optical depletion of dark excitons from a semiconductor quantum dot, Appl. Phys. Lett. **106**, 193101 (2015).

[14] N. S. Jones and T. M. Stace, Photon frequency-mode matching using acousto-optic frequency beam splitters, Phys. Rev. A **73**, 033813 (2006).

[15] X. B. Wang, C. X. Yang, and Y. B. Liu, On-demand entanglement source with polarization-dependent frequency shift, Appl. Phys. Lett. **96**, 201103 (2010).

[16] K. Brunner, G. Abstreiter, G. Böhm, G. Tränkle, and G. Weimann, Sharp-Line Photoluminescence and Two-Photon Absorption of Zero-Dimensional Biexcitons in a GaAs/AlGaAs Structure, Phys. Rev. Lett. **73**, 1138 (1994).

[17] S. Stufler, P. Machnikowski, P. Ester, M. Bichler, V. M. Axt, T. Kuhn, and A. Zrenner, Two-photon Rabi oscillations in a single $In_xGa_{1-x}As$/GaAs quantum dot, Phys. Rev. B **73**, 125304 (2006).

[18] H. Jayakumar, A. Predojević, T. Huber, T. Kauten, G. S. Solomon, and G. Weihs, Deterministic Photon Pairs and Coherent Optical Control of a Single Quantum Dot, Phys. Rev. Lett. **110**, 135505 (2013).

[19] D. Gammon, E. S. Snow, B. V. Shanabrook, D. S. Katzer, and D. Park, Fine Structure Splitting in the Optical Spectra of Single GaAs Quantum Dots, Phys. Rev. Lett. **76**, 3005 (1996).

[20] V. D. Kulakovskii, G. Bacher, R. Weigand, T. Kümmell, A. Forchel, E. Borovitskaya, K. Leonardi, and D. Hommel, Fine Structure of Biexciton Emission in Symmetric and Asymmetric CdSe/ZnSe Single Quantum Dots, Phys. Rev. Lett. **82**, 1780 (1999).

[21] Y. Benny, S. Khatsevich, Y. Kodriano, E. Poem, R. Presman, D. Galushko, P. M. Petroff, and D. Gershoni, Coherent Optical Writing and Reading of the Exciton Spin State in Single Quantum Dots, Phys. Rev. Lett. **106**, 040504 (2011).

[22] E. Poem, O. Kenneth, Y. Kodriano, Y. Benny, S. Khatsevich, J. E. Avron, and D. Gershoni, Optically Induced Rotation of an Exciton Spin in a Semiconductor Quantum Dot, Phys. Rev. Lett. **107**, 087401 (2011).

[23] M. B. Ward, M. C. Dean, R. M. Stevenson, A. J. Bennett, D. J. P. Ellis, K. Cooper, I. Farrer, C. A. Nicoll, D. A. Ritchie, and A. J. Shields, Coherent dynamics of a telecom-wavelength entangled photon source, Nat. Commun. **5**, 3316 (2014).

[24] A. Peres, Separability Criterion for Density Matrices, Phys. Rev. Lett. **77**, 1413 (1996).

[25] M. O. Scully and M. S. Zubairy, *Quantum Optics* (Cambridge University Press, Cambridge, 1997).

[26] E. R. Schmidgall, I. Schwartz, L. Gantz, D. Cogan, S. Raindel, and D. Gershoni, Deterministic generation of a quantum-dot-confined triexciton and its radiative decay via three-photon cascade, Phys. Rev. B **90**, 241411 (2014).

[27] D. F. V. James, P. G. Kwiat, W. J. Munro, and A. G. White, Measurement of qubits, Phys. Rev. A **64**, 052312 (2001).

[28] C. L. Salter, R. M. Stevenson, I. Farrer, C. A. Nicoll, D. A. Ritchie, and A. J. Shields, An entangled-light-emitting diode, Nature (London) **465**, 594 (2010).

[29] H. P. Specht, J. Bochmann, M. Mücke, B. Weber, E. Figueroa, D. L. Moehring, and G. Rempe, Phase shaping of single-photon wave packets, Nat. Photon. **3**, 469 (2009).